Analysis of 3D LiDAR and 1D FMCW Radar Effectiveness for Distance Estimation in Inland Ports for Remote-Controlled Ship Navigation

Fynn Pieper
Institute of Systems Engineering for Future Mobility
German Aerospace Center (DLR)
Oldenburg, Germany
fynn.pieper@dlr.de

Mirjam Bogner
Institute of Systems Engineering for Future Mobility
German Aerospace Center (DLR)
Oldenburg, Germany
mirjam.bogner@dlr.de

Janusz A. Piotrowski
Institute of Systems Engineering for Future Mobility
German Aerospace Center (DLR)
Oldenburg, Germany
janusz.piotrowski@dlr.de

Matthias Steidel
Institute of Systems Engineering for Future Mobility
German Aerospace Center (DLR)
Oldenburg, Germany
matthias.steidel@dlr.de

***Abstract*—Vessel safety during remote-controlled ship navigation (RCSN) is compromised by depth ambiguity when relying solely on 2D camera streams. While radar and LiDAR sensors have been proposed to increase situation awareness, practical performance comparisons for RCSN applications are sparse. This study proposes a practical evaluation of 1D FMCW radar and near-field LiDAR sensors for RCSN, focusing on their effectiveness in distance estimation to static objects within harbor settings. A novel LiDAR processing technique is developed, integrating water-plane filtering and surface normal estimation for robust distance estimation. For evaluation, we conduct sea trials by mounting both sensors on a vessel and systematically compare sensor performance during a prototypic maneuver. Results indicate that radar is less likely distracted by elusive objects, while LiDAR achieves high-resolution sampling with increased accuracy detecting even weak reflecting objects. These findings highlight specific use cases for each sensor in RCSN and provide additional guidance for their optimal deployment to enhance operator situation awareness.**

Keywords—Remote Control, LiDAR, Radar, Distance Estimation, Object Detection, Sensor Comparison, Field Trials

I. Introduction

Recent years have seen significant progress in the automation of maritime navigation partly due to cost reductions, increased safety and a shortage of qualified maritime personnel [1], placing increased focus on remote-controlled ship navigation (RCSN). Pilot projects such as Seafar [2] and FernBin [3] explore how to remotely monitor and operate multiple ships with a reduced crew on board. These projects serve as first steps on the path towards Maritime Autonomous Surface Ships (MASS) improving efficiency, working conditions and sustainability. More generally in RCSN, either one or multiple ships are controlled by a human operator [4] from a Remote Operation Center (ROC) eliminating the need for an experienced crew on board. In this paper, we focus on RCSN both with and without seafarers on board, as described in Degree Two and Three autonomy by the International Maritime Organization (IMO) [5].

By reducing or fully eliminating the crew on board, one may sacrifice the ability to physically interact with the ship in case of emergencies, such as collision threats, thus compromising vessel safety. For this reason, RCSN relies on automated navigation systems to safeguard the ship in absence of a crew. Unlike traditional navigation, where a captain directly observes the ship's environment, RCSN requires dedicated sensors. Each sensor captures specific aspects of the ship's surroundings to inform the remote operator navigating the ship. Still, different sensors have specific advantages and shortcomings when it comes to augmenting human levels of situation awareness [6]. Conventionally, operators of remotely controlled ships rely on high-resolution camera streams that provide live information on the ship's environment [7]. Despite the direct perception of the ship's surroundings, exclusively using two-dimensional image streams may result in ambiguous depth perception [8].

Since the operator's inability to accurately determine distances towards surrounding objects increases the risk of collision with nearby vessels or shore infrastructure, camera streams must be complemented by other sensors, which are able to gauge absolute depth [9]. However, different sensors vary in their ability to extract distance readings from nearby objects in varying conditions, drastically influencing their effectiveness for RCSN. As a result, determining the most appropriate sensor for a specific maritime scenario can be a complex endeavor as it depends heavily on the intended use case. Finding the sensor best suited for any maritime task requires a methodical approach to evaluate the individual sensor's strengths and weaknesses in real-world scenarios.

This paper presents a comprehensive evaluation of radio detection and ranging (radar) and light detection and ranging (LiDAR) for application in RCSN, focusing on their performance in collision avoidance tasks and ability to enhance situation awareness. While the primary contribution lies in the comparison of both sensors within maritime domain and the elaboration of optimal application scenarios, we also develop a novel approach for distance estimation in the maritime domain based on LiDAR data.

II. Remote Sensing In Maritime Applications

While the focus of this study is on the application of remote sensing technologies within maritime systems, it is instructive to look at the more mature automotive domain first. In autonomous driving systems, radar and LiDAR are the most commonly used remote sensing methods to supplement depth information to ambiguous image streams [10 & 11]. Both radar and LiDAR rely on the signal characteristics estimating the distance towards nearby surfaces by measuring the duration of the radio signal and laser impulse, respectively, to return after being emitted. Despite this similarity, LiDAR sensors are still the preferred choice used for autonomous driving demonstrators and fleets of autonomous vehicles [11].

A. Radar Sensors

This selection of sensors cannot directly be transferred to the maritime domain, as the system requirements diverge significantly due to the differing application scenarios [12]. Historically, pulsed radar systems are the preferred choice within the maritime domain as they are robust against harsh environmental conditions. Pulsed radar typically operates in the microwave bands of the radio spectrum (microwave range) enabling radar signals to penetrate fog, rain and snow with minimal signal attenuation and backscatter [13]. High-power marine radars (8-12 GHz; 37 cm wavelength) with 360-degree coverage are used for open sea navigation, providing robust readings over multiple kilometers. However, marine radars must not be used within harbors, as the high-power signal can compromise instruments used by the local vessel traffic service (VTS) [14]. As a consequence, many works adopt high-resolution radars (60-110 GHz; 4 mm wavelength) used in autonomous vehicle applications [15 & 16].

One example is frequency-modulated continuous-wave (FMCW) radar, which have a lower power output and are safe to use within harbor settings. These radars rely on electronic scanning phased arrays without mechanical movement, achieving higher axial and lateral resolutions [17]. FMCW radars therefore allow for sharper object distinction and better targeting, enhancing detection and tracking for larger objects [18] and maritime infrastructure [19]. This is often assisted by FMCW radar's capability to measure the difference in transmitted and received frequency (Doppler shift), which is used to gauge the radial velocity of the detected object. Combining distance and velocity measurements can significantly decrease radar track uncertainty of moving objects [20], which is of particular interest for real-time collision avoidance tasks [21].

However, FMCW radar's operating principle also imposes constraints on its performance. Notably, FMCW radars have a limited field-of-view (FOV). This limitation is a result of the horizontal radiation pattern of typically less than 15 degrees, which is too restrictive for many maritime applications where wide coverage is essential [17]. To counteract these limitations, some systems integrate multiple radars achieving a greater coverage for tasks such as ship navigation and berthing assistance [22]. Still, the lower power output of high-resolution radars generally reduces their operational ranges and makes them increasingly susceptible to environmental conditions, leading to impaired performance in adverse weather or strong undulation. While increasing the carrier frequency can slightly improve range and robustness [19], doing so causes a reduction in resolution.

Notably, radar performance also heavily depends on the object's radar cross-section (RCS), which is mainly determined by the object's material and size. As a consequence, small objects tend to be harder to detect [23], presenting a particular challenge in densely populated environments with both large and small objects such as harbors. Similarly, wooden harbor structures (e.g. pilings, dolphins or piers) cause weak radar reflections making them more elusive compared to steel structures [24]. Some approaches increase RCS of wooden objects by mounting radar reflectors on top of the object [21 & 24], thus improving reflection properties. Generally, radar presents a highly versatile sensor within maritime environments used for object detection and tracking tasks.

B. LiDAR Sensors

In contrast to radar, LiDAR sensors are less common in the maritime domain as they emit concentrated light beams in the infrared spectrum (near-infrared range; 850-1550 nm wavelength). This shorter wavelength inherently makes LiDAR more susceptible to interference from adverse weather conditions, such as fog, rain and snow [25] and physical obstructions. Even in the absence of adverse conditions detection performance may be affected by glare from the sun. Nonetheless, practical tests under real conditions, demonstrate how these effects can often be mitigated by applying appropriate filtering techniques [26].

Due to its narrow laser beam width, LiDAR achieves high precision measurements. Unlike high-resolution radars that continuously scan an area, LiDAR uses laser pulses to sample discrete directions and measure the distance to the next surface with high vertical and horizontal resolution. Grouped together, the resulting data points discretize the 3D environment of the LiDAR into a point cloud. In addition to an increased resolution the combination of the shorter wavelength and the short pulse duration makes individual measurements more distinctive improving depth sampling. Just as with marine and high-resolution radar sensors, different types of LiDAR sensors are available. Survey-grade LiDAR systems for terrestrial scanning are typically a lot more powerful with operational ranges of up to multiple kilometers. However, the long scan time is not suited for dynamic environments distorting scans [27].

Assistance systems for situational awareness and reactive decision-making are typically based on LiDAR systems from the automotive domain, as a result of their low cost and faster scanning intervals. These near-field LiDAR have operational ranges of up to a few hundred meters while maintaining a high resolution and excel in applications that require precise spatial awareness, such as autonomous berthing [28 & 29] or navigation in congested waters [30]. Applications unique to LiDAR include high-accuracy maritime mapping [31] and subsequent infrastructure inspection [32]. However, due to the extensive nature of point cloud data, the data processing involved in handling LiDAR point clouds requires significantly more computational resources when compared to radar. For this reason, many works down-sample [26 & 28] or filter measurements according to the use case, e.g. eliminating sky, water or the sensor carrier itself [33]. Measuring distances with precise angular placement, LiDAR is able to detect small objects and effectively complements camera data, especially in near-field, cluttered environments [34].

In summary, LiDAR is able to generate high-resolution 3D point clouds of its surroundings with great coverage. Due to its limited range and susceptibility to weather conditions, LiDAR is best suited for target detection and shape identification tasks for nearby targets within calm harbor conditions.

C. Demand for Practical Sensor Performance Comparison in Maritime Environments

Despite the work put into the individual analysis of high-resolution radar and near-field LiDAR sensors for close-range maritime application, many omit a comprehensive evaluation tied to the specific use case of RCSN. While studies such as [9 & 11] acknowledge theoretical sensor differences and propose application guidelines based on operating principles, they cannot model real conditions resulting in a lack of practical relevance to RCSN.

In [35], the authors acknowledge the importance of practical testing, but only analyze indoor scenarios. Other works formulate the problem as a self-localization problem in near-shore environments and recognize the complementary nature of radar and LiDAR by integrating both sensors [36] but do not provide an ablation study. To demonstrate the practical differences in the use of high-resolution radar and LiDAR technology employed for RCSN, a practical field study is needed to evaluate the effectiveness of both sensors in estimating the distance to dynamic and static obstacles. For this study, we will focus on the practical estimation performance towards static harbor infrastructure.

While both sensor modalities are generally capable to estimate the distance to static infrastructure, we aim to identify the characteristics that are relevant to safeguarding RCSN and to highlight optimal use cases. To achieve this, we will conduct a comprehensive practical evaluation of each sensor to provide a realistic comparison of their performance. This study seeks to examine the differences in real-world effectiveness between high-resolution radar and near-field LiDAR sensors for estimating obstacle distances in harbor environments when subjected to standardized pre-processing techniques, while exploring the implications for optimizing sensor deployment in RCSN. By addressing these aspects, this paper aims to establish a basis for informed sensor selection.

III. Sensor Data Processing

To ensure fair comparison, we collect data from both sensors and subject them to comparable pre-processing steps to obtain distance measurements. This way, we ensure that the observed performance differences can be largely attributed to inherent sensor characteristics.

A. Radar processing

Radar data processing is performed according to [37] estimating the distance to a static harbor quay based on one-dimensional FMCW radar data. This work integrates a combination of filtering and clustering techniques aimed at enhancing distance estimation of FMCW radar to static obstacles. Initially, unprocessed radar measurements are filtered to exclude signals that do not meet specific criteria.

Specifically, measurements with a signal strength below a minimum threshold or with a radial velocity exceeding a maximum limit are excluded. Additionally, isolated measurement without nearby data points are discarded, resulting in robust and relevant selection of remaining data points. Subsequently, the authors assessed the effectiveness of three distinct clustering techniques in refining the radar data.

Given that their results indicate only marginal differences in performance, we choose to implement the computationally least complex method, Density-Based Spatial Clustering of Applications with Noise (DBSCAN) with a maximum neighborhood radius for clustering points of $\varepsilon = 1.5$ and $min\_samples = 10$. DBSCAN is particularly adept at managing varying cluster densities without prior knowledge of cluster count, which comes in beneficial in cluttered harbor environments. The final distance to the quay is determined by selecting the two largest clusters and calculating the weighted average distance per cluster. The smaller of both distances is then used for collision avoidance. This choice reflects a safety perspective, as the shorter distance represents a greater safety risk, even if it belongs to the smaller or less prominent cluster.

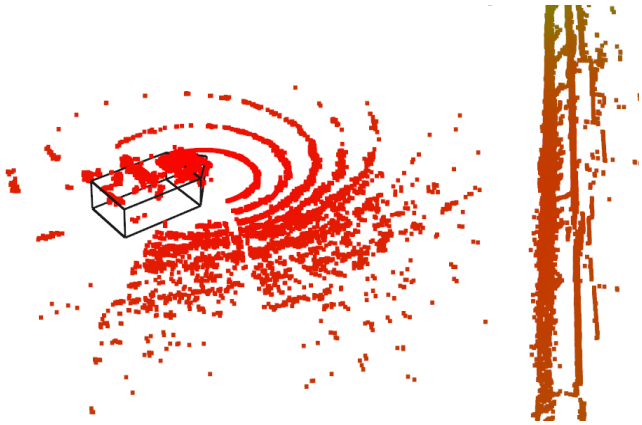

Fig. 1: The vessel is shown as a black wireframe together with the LiDAR data in red. On the right side of the image, harbor structure is captured, while many undesired water reflections are sampled around the vessel.

B. LiDAR processing

Unlike FMCW radar, LiDAR surveys specific directions, precisely mapping each laser's impact location in 3D space. This shifts data processing from intensity-based clustering to analyzing spatial context. As shown in Fig. 1, the 360-degree FOV of the LiDAR captures irrelevant measurements, such as own-vessel hits or water reflections, that do not contain any information about the harbor infrastructure. Since the LiDAR is fixed on the ship's bow, we can eliminate own-vessel hits using a box filter to capture only the surrounding area. Unlike filtering roads for cars, filtering the water surface in the maritime domain is a major challenge. Large roll angle variations complicate consistent estimation, while the erratic behavior of waves challenges the estimation over time.

We then remove water surface reflections near the boat as they contain no information relevant for collision avoidance tasks. Instead of using a voxel grid as in [26 & 28], we use a kd-tree to efficiently search the point cloud data by pruning irrelevant parts. Building on [38], we identify all points corresponding to the water surface by fitting a plane to the measurements near the boat and removing them. We apply the Random Sample Consensus (RANSAC) [39] method to estimate the plane equation, which can be described as

$$p_{water}: Ax + By + Cz + D = 0.$$

Here, x, y and z are the coordinates along the three Cartesian axes within the vessel coordinate system. The plane's orientation relative to the vessel is determined by the corresponding normal vector $\vec{n}_{water} = (A, B, C)^T$. RANSAC was chosen as an effective strategy to fit a plane through the water reflections around the vessel, while dampening the impact of outliers, caused by obstacles such as nearby buoys without requiring IMU data. Including a larger area for plane estimation further improves the exclusion of local outliers. However, including too large areas may cause problems when the vessel travels near large objects, as these might be assumed as parts of the water surface and skew the plane estimation.

During the plane fitting process, the average vertical distance from each water surface measurement to the water plane is recorded, providing a reference distance for the wave height. This distance is used as a threshold to dynamically reflect the roughness of the sea surface and to discard all points that are either close to the water surface or lie beneath, thereby eliminating any water reflections. After preprocessing the point cloud, we analyze its spatial arrangement and deduce the local orientation of the sampled surfaces.

To approximate the normal direction at each point, we calculate the surface normal of the plane tangent to the local surface formed by surrounding data points, as described by the mathematical equations in [40]. Note, that the direction of the estimated surface normal is always on half of the sphere in the Extended Gaussian Image, always facing towards the sensor. To ensure structural consistency, we specify

$$\vec{n}_i \cdot \left(v_p - p_i\right) > 0 \tag{1}$$

with $\vec{n}_i$ being the point normal direction based on the view-point v_p (being the LiDAR origin) and all points p_i in Fig. 2.

Also, under the assumption that man-made structures typically protrude vertically from the water, all surfaces with a normal direction parallel to the water surface are considered for distance estimation. Therefore, we stipulate a maximum angle between $\vec{n}_{water}$ and $\vec{n}_i$ of θ = ± 10 degrees, based on the average accuracy of surface approximation by the chosen method. So, for every point on a vertical surface

$$|\, \vec{n}_{water} \cdot \vec{n}_i \,| \geq \cos(\theta) = 0.985 \tag{2}$$

applies. Focusing only on vertical surfaces ensures robust distance measurement to harbor structures and vessels. By excluding misaligned points, LiDAR accuracy improves by reducing environmental interference from spray and waves. The shortest distance to harbor structures is determined independent form the sensor position using a coordinate transform. This allows to measure the distance from the vessel's center or the outermost corners.

IV. Field Test Design

In existing literature, the comparison between LiDAR and radar technologies often remains theoretical or inadequately applied to maritime environments, e.g. harbors. We address this gap by providing a comprehensive real-world evaluation of both technologies, focusing specifically on their performance in distance estimation for collision avoidance.

A. Experimental Setup

The field trials were conducted in the Jarßum harbor of Emden, using the research vessel "Sally" from the e-Maritime Integrated Reference Platform[1] [41, 42] as sensor carrier. The vessel was equipped with a Saab R5 Supreme DGNSS NAV System for geolocalization purposes. The GPS receiver has an update frequency of 1 Hz and a specified position accuracy below 0.4 meters, corroborated by test results obtained in [37].

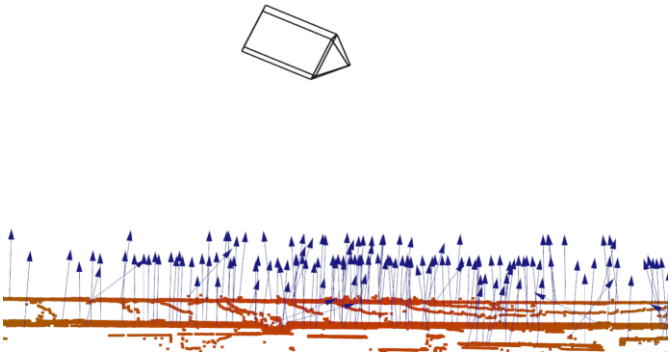

Fig. 3: Birds-eye view on the vessel, the point cloud data (red dots) and the estimated normal directions (blue arrows) of the harbor quay. The vessel is navigated along the quay. Each fiftieth point normal is shown for clarity, most of which are oriented parallel to the water surface.

Additionally, three SICK RMS1000 radars, as proposed by [37], are placed on the bow, in a 45° angle and on the right side of the ship's railing. Although the horizontal FOV is limited to ±60° the sensors are configured with a horizontal and vertical FOV of ±10° and ±4° respectively. Narrowing the FOV is necessary to localize the direction of reflections with 1D sensors. The manufacturer specified operating range lies between 0.4 m and 100 m with an accuracy of 0.04 m and the frequency modulated between 61 to 61.5 GHz. Measurements are acquired at a rate of 10 Hz. While the radars are set to a horizontal FOV of 10°, they can only measure radial distance, doppler shift and amplitude of the return signal and do not provide azimuth or elevation angles. Therefore, the three radars are combined into a larger system, as proposed by [18].

Lastly, a Velodyne VLP-32C LiDAR sensor is mounted in the center of the vessel's bow. The horizontal and vertical FOV are specified by the manufacturer to be 360° and 40° (-25° to +15°), respectively. The operating range lies between 0.1 m and 200 m at 90% reflectivity with an accuracy of ±3 cm. We use the "Strongest" Return Mode with rotation speed set to 600 revolutions per minute, aligning with the FMCW radar settings producing measurements with a horizontal resolution of 0.2° at 10 Hz. We select the size of the area around the ship considered for water plane estimation based on the application scenario. Since the vessel is expected to be maneuvered at least ten meters from the quay at all times, we set the radius for water plane estimation to r_{water} = 10 m. To ensure a precise positioning of all sensors, the vessel's outer dimensions as well as the positions of the DGNSS, radar and LiDAR relative to the vessel were determined using a 3D Real-Time Kinematic (RTK) GPS geo-Fennel FGS 150-L with an accuracy of < 5 mm + 0.5 ppm RMS.

B. Sea Trial Design

The experiment was adopted from [37] to ensure comparability and explore discrepancies in spatial and depth detection characteristics between radar and LiDAR systems. During the prototypic maneuver, shown in Fig. 3, the vessel was maneuvered 100 meters away from a quay wall, starting with its bow facing orthogonally towards the quay. The vessel then accelerated towards the quay to 5 knots, maintaining its course until the distance was reduced to about 20 meters. At this point, the vessel executed a 90-degree turn to port, taking

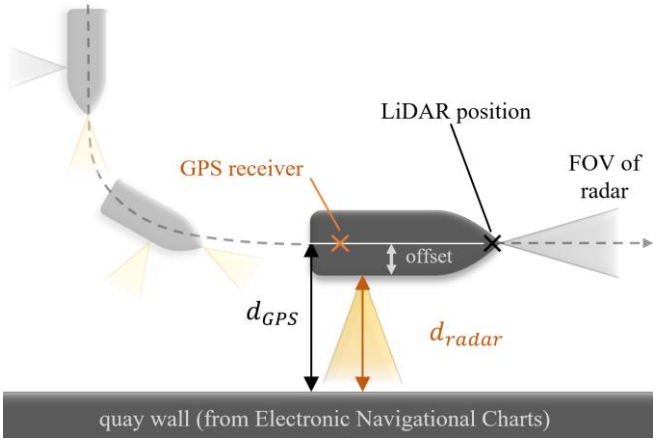

Fig. 2: Illustration of the sea trial maneuver for evaluating LiDAR and radar sensor data processing. The vessel approaches the quay wall, executes a 90-degree portside turn, and then continues parallel to the quay for 100 meters. The LiDAR sensor is mounted on the vessel's bow, and the radars are positioned along the railing.

[1] https://emaritime.de/

a new course parallel to the quay wall, and maintaining this orientation for another 100 meters. The maneuver was repeated six times with varying distances from the harbor quay. Both sensor systems recorded data throughout the maneuver, which was analyzed to determine performance for different distances between vessel and harbor objects is examined.

Temporal alignment of DGNSS, radar, LiDAR and the servers for sensor data collection is ensured using Network Time Protocol (NTP). For evaluation of the trails we rely on the official Electronic Navigational Charts (ENC) of the harbor Emden provided by the Federal Maritime and Hydrographic Agency of Germany (BSH). These charts are standardized navigation reference for mariners. The sea trials were conducted at noon under clear weather conditions, with direct sunlight and excellent visibility. The wind speed averaged 10 knots[2], resulting in calm harbor waters with few waves.

V. Results and Discussion

Consistent with our research aims, the collected data are examined using qualitative considerations and quantitative metrics, thus incorporating practical observations and objective data. Specifically, the qualitative evaluation of the sensor data tries to identify differences in the behavior performance of both methods. Conversely, the quantitative analysis focuses on objective evaluation metrics to assess the performance of both sensor systems, without subjective bias.

A. *Qualitative Analysis*

While we present results for one maneuver, stated findings are representative for all maneuvers. The collected sensor data are depicted in Fig. 4 as distance over the duration of the maneuver, showing the vessel closing in on the quay as well as the parallel maneuvering along the quay. Looking at the radar sensors, at first the front radar effectively estimates the shortest distance to the quay. Closing in on 20 seconds, the vessel turns and the limited FOV of the front radar no longer captures the whole quay so that the radar can no longer estimate the shortest distance correctly. However, the second sensor, which is mounted in a 45° angle, correctly detects the quay for a few seconds, before the portside sensor produces the shortest distance estimate. The combination of the three radar sensors does not create any evident blind spots.

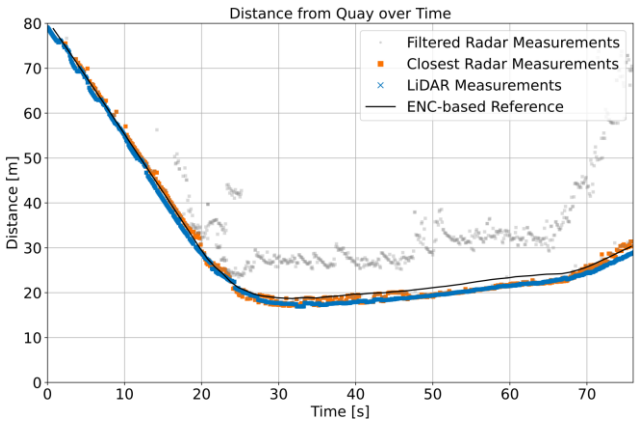

Fig. 4: Plot of the distance to the quay wall during one maneuver. It can be seen that both radar and LiDAR filter out noise effectively. While the front radar sensor loses sight of the quay during turning, the angled radar sensor takes over and is able to estimate the distance to the quay more accurately.

Fig. 5: Harbor quay with concrete bulwark and wooden planking. The bulwark is protruding 1.8m from the charted quay wall.

During the whole maneuver, both sensor systems consistently reflect the ground truth, though the LiDAR consistently reports slightly too low distance values. After the turn, the radar sensor also occasionally provides distance values that are slightly too short. Zooming in on the evaluation data, Fig. 5 shows radar to more accurately estimate the quay wall position than LiDAR. However, looking at the radar estimations, two distinct distances seem to come up frequently. Firstly, the distance towards the official quay wall position marked in black, and secondly, another distance, which is 1.7 meters shorter. We highlighted this distance by the red dashed line. Evidently, this line approximates the LiDAR data well, hinting towards another surface, which was consistently detected by both sensors during the parallel maneuvering. After thorough inspection, we find, that the closer object is a wooden planking on a bulwark extending from the quay, shown in Fig. 5, which is not charted in the ENCs. Even though the bulwark is not charted, it has significant impact on the distance estimation, as it presents the closest object, with the highest risk of collision. However, the less reflective surface of the wooden planks causes the FMCW radars to focus on the highly-reflective metal surface of the quay. This is a consequence of the processing approach chosen by [37], which filters low-amplitude radar measurements.

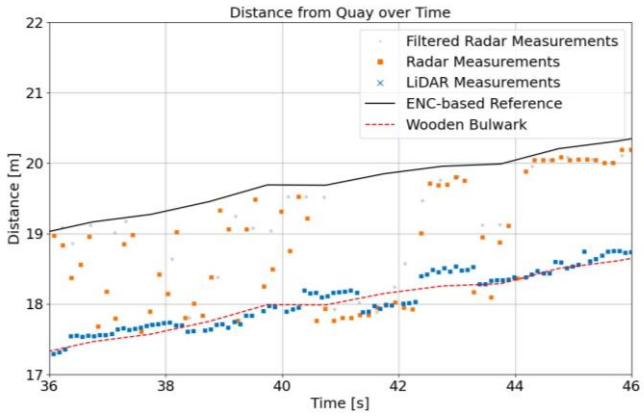

Fig. 6: Zoomed in section of Fig. 5. Also, a dashed line in red was added, indicating a distance at which both radar and LiDAR detect the wooden planks on the bulwark.

[2] https://meteostat.net/de/station/10203?t=2024-05-13/2024-05-13

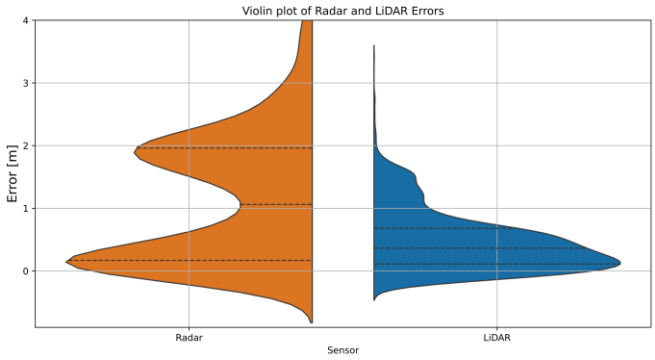

Fig. 7: Violin chart comparison of radar and LiDAR estimation errors. The peaks in the radar data mainly stem from the metal quay and the wooden planking, while the LiDAR detections are caused by the wooden bulwark.

Critical misjudgments arise, when readings from the closest object are overshadowed by other objects that are farther away but have a larger RCS, such as the metal quay. In this case, exaggerated weighing of highly reflective objects can be avoided using a 3D LiDAR sensor, since spatial analysis is likely more robust in the presence of less reflective surfaces which impede signal strength assessment.

B. Quantitative Analysis

For an in-depth comparison of all maneuvers, we consider the combined distribution of absolute errors in Fig. 7, which depicts an asymmetrical violin chart illustrating the data's spread and skewness as well as median and interquartile ranges. The plot is generated using a kernel density estimate based on Scott's Rule to smooth the probability density of the data and show its distribution. Similar to the qualitative observations, the highest peaks of both violin charts align with the bulwark, indicating an accurate detection in most cases. The radar violin chart shows a wider distribution of errors with a heavier tail extending towards the positive values, indicating a tendency to overestimate distances. As discussed before the second peak at approximately 1.7 m is caused by the high reflectivity of the metal quay wall, while measurements from even farther are the result of metal objects on top of the quay. On the other hand, LiDAR measurements are concentrated around the desired distance of the bulwark with a shorter tail towards positive values, which is a result of quay estimations, when the vertical resolution restricts bulwark detections. These effects can also be found in the error over distance in Fig. 8. Both sensors have problems estimating the distance to the bulwark when the vessel is approaching the quay, but recover when closing in on the bulwark during the portside maneuver.

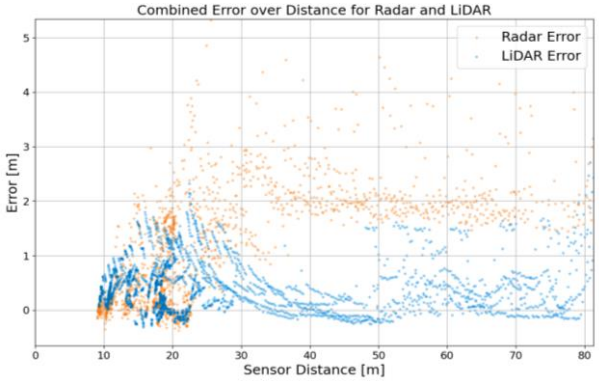

Fig. 8: Error in distance to bulwark during all maneuvers. LiDAR errors closely align with the bulwark at all distances, despite detection problems at specific ranges resulting from a limited vertical resolution. Radar only detects the bulwark at shorter distances. Beyond 30 m, radar primarily perceives the metal quay, as indicated by the consistently larger error.

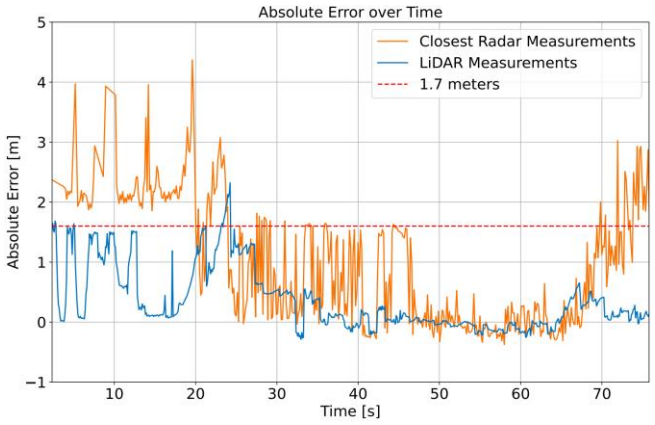

Fig. 9: Estimation error towards bulwark during a representative maneuver.

As shown in Fig. 9, accuracy of both sensors is significantly improved when the vessel is navigated parallel to the quay as the distance is reduced. While radar estimations still skip back and forth between the steel quay and the wooden planking on the bulwark, the LiDAR is reliably detecting the wooden surface. Also, LiDAR measurements are more stable, resulting in a less noisy signal despite failing to correctly estimate the water surface in one maneuver as the vessel was too close to the quay.

Further, we introduce five objective metrics to offer different perspectives on sensor performance. The average distance error (δ_{av}) captures the overall sensor accuracy, while the maximum distance errors (δ_{max}) showcases the worst-case scenario, ensuring insights into both general reliability and estimation stability. The root mean squared error ($RMSE$) is used to assess the overall error distribution by penalizing outliers to offer a more realistic representation of potential operational risks. Lastly, the signal-to-noise ratio (SNR) is calculated as to assess the sensor's ability to function in noisy maritime environments using

$$SNR = 10 * \log_{10}\left(\frac{S^2}{N^2}\right) \quad (3)$$

where signal (S) is the chosen measurements intensity and noise (N) the average intensity of the filtered measurements. Metrics are shown in Table 1 as average for all maneuvers.

Evidently, the LiDAR outperforms radar when looking at estimation accuracy. Both average and worst-case performance are enhanced as a result of high radial resolution and its capability of spatial analysis. While corroborated by the lower RMSE, the similar ratio between average distance error and RMSE of both sensor system is suggesting a comparable error distribution. As indicated in the related work, radar achieves a higher average SNR, leading to clearer signal differentiation from clutter based on intensity alone.

Table 1: Average metrics with standard deviation for distance estimation towards the bulwark for all maneuvers. The arrows indicate the optimal outcome for each metric.

Metric	**Radar [36]**	**LiDAR**
δ_{av} [m] ↓	1.1 ± 0.1	**0.42 ± 0.03**
δ_{max} [m] ↓	4.5 ± 1.15	**2.23 ± 0.67**
RMSE [m] ↓	1.59 ± 0.13	**0.66 ± 0.04**
SNR [dB] ↑	**22.21 ± 0.32**	15.62 ± 1.28

C. Summary and Recommendations

The evaluation of radar and LiDAR systems under controlled conditions shows that both sensors are generally capable of estimating the distance to nearby objects and can be used for collision avoidance in RCSN applications. However, key performance differences became apparent, indicating unique strengths, limitations and potential application scenarios for each sensor.

Radar is known for its robustness in adverse weather but was not able to maintain a high SNR in our tests. Due to the wide spatial coverage, relevant structures could be recognized in time, but the exact position of the object remained vague. While the FMCW radar's detection accuracy was generally high, it was compromised in the presence of highly reflective surfaces. This can be seen from the fact that the highly reflective metal quay overshadowed the wooden bulwark, which was located closer to the boat and, if overlooked, could lead to serious accidents. This trade-off can be viewed as both an advantage or a disadvantage. In cluttered environments, this form of prioritization can filter out irrelevant, weak detections allowing the primary target to be identified more clearly. An example of this would be the detection of a sailing boat among debris in the harbor. On the other hand, this characteristic becomes disadvantageous if the object to be detected is not sufficiently distinct or may even reflect only a weak signal. This might be the case for wooden structures, like the planking on the bulwark in our tests, or small obstacles in the harbor, such as a swimming person.

As a result of radar's heavy dependency on return signal strength, objects with a larger RCS are favored. With regard to RCSN this means, that FMCW radar sensors are most effective in the detection and distance estimation towards large, well-reflecting objects, such as metal structures, most harbor infrastructure or ships. FMCW radar may be used to guide ships and help them safely approach docks or harbor walls in fog, rain, or during nighttime, where visual cues from camera streams are limited. However, to use FMCW radar for small or poorly reflective objects, radar reflectors can be fitted to these objects to increase their RCS as mentioned by [24].

Here, our findings challenge conventional assumptions by showing that LiDAR achieves a higher reliability than FMCW radar in cluttered maritime environments under test conditions. Its ability to sample whole scenes with high resolution allows it to detect even small objects with poor reflectivity, correctly capturing quay and bulwark. Despite the lower SNR, indicating ambiguous signals, the spatial data analysis was able to eliminate dependence on amplitude, but still necessitates elaborate processing. Still, test results were limited by the vertical resolution of the used LiDAR which caused inconsistent detection of the shallow bulwark at greater distances. These effects are corroborated by the qualitative evaluation and are reliably reproducible.

Our tests indicate that LiDAR is the preferred choice for advanced RCSN which requires spatial differentiation, capturing even small cues from the environment to make well-informed decisions. This is the case for navigation in congested waterways with many participants of different sizes. Similarly, the increased spatial resolution allows operators or algorithms to gain a broader understanding of the scene, which can be used for docking maneuvers including the automated detection of small mooring bollards as in [43]. By integrating radar and LiDAR into a complementary system, we hypothesize that the distinct advantages of each sensor can be leveraged to enhance estimation performance in diverse maritime scenarios. The aim is to use radar's ability to maintain stable estimation results even in challenging weather conditions as well as LiDAR's high spatial resolution and accuracy for detailed scene understanding. Combining both sensor modalities into a single hybrid system enhances detection accuracy under varying conditions and increases robustness through sensor redundancy. Sensor redundancy will enhance operational safety by reducing the risk of total system failure in case of single-sensor malfunction. Overall, a hybrid approach could address the limitations of each individual sensor and present a more versatile and adaptive system for RCSN.

VI. CONCLUSION

The ongoing trend of automation in maritime navigation aims to reduce on-board crews by placing increased focus on remote-controlled ships. This transition requires versatile and robust assistance systems to substitute human levels of perception for the remote operator to make decisions upon. By comparing distance estimation performance of 1D FMCW radar and 3D LiDAR systems towards harbor objects, this paper gives a practical overview over sensor behavior in harbor settings.

Specifically, achieved results demonstrate that FMCW radar is an effective sensor for efficient distance estimation and collision avoidance in noisy or cluttered environments but may struggle with low-reflective or small objects due to its beam divergence and dependence on strong signal reflections. Latter particularly impeded distance estimation towards wooden structures with a low radar cross section. In contrast, test results suggest that LiDAR provides more sophisticated environment detection for deduction tasks. Based on its extensive field-of-view, high spatial resolution and narrow beam width, our tests demonstrate that LiDAR excels in capturing harbor environments with high accuracy, corroborating its suitability for mapping and scene understanding applications. Nevertheless, LiDAR exhibits a high sensitivity to data processing quality, heavily influencing estimation results. Building on complementary strengths of both sensors, a hybrid system could offer a more versatile and adaptive assistance system for remote-controlled ships combining radar's stability with LiDAR's spatial resolution.

Future research may explore methods to ensure that radar and LiDAR detections remain consistent over time, which would help improve the stability of detection results. By implementing temporal consistency checks more reliable and continuous mapping of the maritime environment can be achieved by verifying that objects are detected in the same way across different moments. Also, the implementation and evaluation of a hybrid system is desirable, as these systems are likely to outperform single-sensor based systems.

VII. ACKNOWLEDGEMENT

The research leading to these results has been carried out under the guidelines of the BMWK and was started in January 2022 within the German Aerospace Center (DLR). We sincerely appreciate the support provided by DLR throughout the project.

VIII. REFERENCES

[1] BIMCO/ICS (2021) Seafarer Workforce Report - The global supply and demand for seafarers in 2021.

[2] SEAFAR. Seafar Remote Navigation. At https://seafar.eu/.

[3] Bejaoui, A., & Söffker, D. (2023). Situated and event discrete decision making support system applied to remotely operated vehicles. In European Safety and Reliability Conference.

[4] Carey, L. (2024). Pushing the Limits: How Limitation of Liability Will Apply to Maritime Autonomous Surface Ships.

[5] IMO, M. (2021). Outcome of the Regulatory Scoping Exercise for the Use of Maritime Autonomous Surface Ships (MASS).

[6] Endsley, M. R. (2018). Automation and situation awareness. In Automation and human performance. CRC Press.

[7] DNV-GL (2018). Remote-Controlled and Autonomous Ships. Group Technology & Research, Position Paper 2018.

[8] Amarasinghe, S., Kodikara, N. D., & Sandaruwan, D. (2014, December). Location estimation in a maritime environment using a monocular camera. In IEEE International Conference on Advances in ICT for Emerging Regions.

[9] Jokioinen, E., Poikonen, J., Hyvönen, M., Kolu, A., … & Makkonen, H. (2016). Remote and autonomous ship—The next steps. Rolls Royce PLC. AAWA Position Paper.

[10] Dayananda, B. N., Srivastava, N., Achala, G., Nandagiri, A., Srihari, P., Pardhasaradhi, B., & Cenkeramaddi, L. R. (2024). Depth Information Fusion Using Radar-LiDAR-Camera Experimental Setup for ADAS Applications. In IEEE Communication Systems and Network Technologies (CSNT).

[11] Bilik, I. (2022). Comparative analysis of radar and lidar technologies for automotive applications. IEEE Intelligent Transportation Systems Magazine.

[12] Brinkmann, M., Böde, E., Lamm, A., Vander Maelen, S., & Hahn, A. (2017). Learning from automotive: Testing maritime assistance systems up to autonomous vessels. IEEE OCEANS.

[13] Zang, S., Ding, M., Smith, D., Tyler, P., Rakotoarivelo, T., & Kaafar, A. (2019). The impact of adverse weather conditions on autonomous vehicles. IEEE vehicular technology magazine.

[14] Lazarowska, A. (2021). Review of collision avoidance and path planning methods for ships utilizing radar remote sensing. In Remote Sensing.

[15] Gusland, D., Torvik, B., Finden, E., Gulbrandsen, F., & Smestad, R. (2019). Imaging radar for navigation and surveillance on an autonomous unmanned ground vehicle capable of detecting obstacles obscured by vegetation. In IEEE Radar Conference.

[16] Zhu, Y., Zhu, Y., Zhang, Z., Zhao, B. Y., & Zheng, H. (2015). 60GHz mobile imaging radar. Workshop on Mobile Computing Systems and Applications.

[17] Ruiz, A. R. J., & Granja, F. S. (2009). A short-range ship navigation system based on ladar imaging and target tracking for improved safety and efficiency. IEEE Transactions on Intelligent Transportation Systems.

[18] Sun, S., Lyu, H., Gao, Z., & Yang, X. (2024). Grid map assisted radar target tracking in a detection occluded maritime environment. In IEEE Instrumentation and Measurement.

[19] Halai, S., Brennan, P. V., Patrick, D., & Weller, I. (2014). Frequency shifted active target for use in FMCW radar systems. In IEEE Radar Conference.

[20] Kufoalor, D. K. M., Wilthil, E., Hagen, I. B., Brekke, E. F., & Johansen, T. A. (2019). Autonomous COLREGs-compliant decision making using maritime radar tracking and model predictive control. In IEEE European Control Conference.

[21] Wilthil, E. F., Flåten, A. L., Brekke, E. F., & Breivik, M. (2018). Radar-based maritime collision avoidance using dynamic window. In IEEE aerospace conference.

[22] Huang, Y., Brennan, P. V., Patrick, D., Weller, I., Roberts, P., & Hughes, K. (2011). FMCW based MIMO imaging radar for maritime navigation. In Electromagnetics Research.

[23] Guo, X., Bai, H., Li, Y., Shui, L., Su, J., & Wang, L. (2024). Small target detection in sea clutter using dominant clutter tree based on anomaly detection framework. In Signal Processing.

[24] Stateczny, A., Kazimierski, W., Burdziakowski, P., Motyl, W., & Wisniewska, M. (2019). Shore construction detection by automotive radar for the needs of autonomous surface vehicle navigation. ISPRS International Journal of Geo-Information.

[25] Zhang, Q., Wang, L., Meng, H., Zhang, Z., & Yang, C. (2024). Ship Detection in Maritime Scenes under Adverse Weather Conditions. In Remote Sensing.

[26] Burnett, K., Wu, Y., Yoon, D. J., Schoellig, A. P., & Barfoot, T. D. (2022). Are we ready for radar to replace lidar in all-weather mapping and localization?. IEEE Robotics and Automation Letters.

[27] Mandlburger, G., Kölle, M., Pöppl, F., & Cramer, M. (2023). Evaluation of Consumer-Grade and Survey-Grade UAV-LIDAR. In Remote Sensing and Spatial Information Sciences.

[28] Hu, B., Liu, X., Jing, Q., Lyu, H., & Yin, Y. (2022). Estimation of berthing state of maritime autonomous surface ships based on 3D LiDAR. In Ocean Engineering.

[29] Mentjes, J., Wiards, H., & Feuerstack, S. (2022). Berthing assistant system using reference points. Journal of Marine Science and Engineering.

[30] Perera, L. P., Oliveira, P., & Soares, C. G. (2012). Maritime traffic monitoring based on vessel detection, tracking, state estimation, and trajectory prediction. IEEE Transactions on Intelligent Transportation Systems.

[31] Sawada, R., & Hirata, K. (2023). lidar. Journal of Marine Science and Technology.

[32] Thoms, A., Earle, G., Charron, N., & Narasimhan, S. (2023). Tightly coupled, graph-based dvl/imu fusion and decoupled mapping for slam-centric maritime infrastructure inspection. IEEE Journal of Oceanic Engineering.

[33] Thombre, S., Zhao, Z., Ramm-Schmidt, H., García, J. M. V., Malkamäki, T., ... & Lehtola, V. V. (2020). Sensors and AI techniques for situational awareness in autonomous ships: A review. IEEE Intelligent Transportation Systems.

[34] Wang, Z., & Zhang, Y. (2022). Estimation of ship berthing parameters based on Multi-LiDAR and MMW radar data fusion. In Ocean Engineering.

[35] Gim, H., Baek, S., Park, J., Lee, H., Sung, C., Kim, K., & Han, S. (2022). Suitability of various LiDAR and radar sensors for application in robotics: A measurable capability comparison. IEEE Robotics & Automation Magazine.

[36] Mounier, E., Dawson, E., Elhabiby, M., Korenberg, M., & Noureldin, A. (2023). Investigating the Complementary Use of Radar and LIDAR for Positioning Applications. In Remote Sensing and Spatial Information Sciences.

[37] Bogner, M., Pieper, F., Steger, C., Steidel, M., Piotrowski, J. A. & Feuerstack, S. (2024). Utilizing 1D FMCW Radar Data for Distance Estimation to Port Infrastructure. In IEEE International Conference on Information Fusion.

[38] Canaz, S., Karsli, F., Guneroglu, A., & Dihkan, M. (2015). Automatic boundary extraction of inland water bodies using LiDAR data. In Ocean & Coastal Management.

[39] Fischler, M. A., & Bolles, R. C. (1981). Random sample consensus: a paradigm for model fitting with applications to image analysis and automated cartography. ACM.

[40] Rusu, R. B. (2010). Semantic 3D object maps for everyday manipulation in human living environments. Künstliche Intelligenz.

[41] Rüssmeier, N., Lamm, A., & Hahn, A. (2019). A generic testbed for simulation and physical-based testing of maritime cyber-physical system of systems. Journal of Physics: Conference Series. IOP Publishing.

[42] Piotrowski, J. A., Steger, C., & Hahn, A. (2025). Open testbed vessel—Reusable and generic test carrier architecture for maritime testbeds. Ocean Engineering, 325, 120747.

[43] Jindal, M., Jha, A., & Cenkeramaddi, L. R. (2021). Bollard segmentation and position estimation from lidar point cloud for autonomous mooring. IEEE Geoscience and Remote Sensing.